Imperial College London

Department of AERONAUTICS

Profile Drag and Wake Momentum Deficit Lab Report

Lab Group 07: Himmat Kaul, Brendan Frain, Emre Aslan, Yujie Hao, Suhail Halaby, Nicolas Zhou.
CID: 02376386

5th December 2024

Contents

List of Figures

List of Tables

List of Symbols

v	Tunnel Velocity
T	Temperature
ρ_{air}	Air Density
$\rho_{ethanol}$	Ethanol Density
P_a	Ambient Pressure
x	Chordwise Direction
y	Thickness Direction
x/c	Non-Dimensional Chord
y/c	Non-Dimensional Thickness
y_w	Wake profile coordinates
c	Chord Length
Re	Reynolds Number
M	Mach Number
C_D	Drag Coefficient
C_{D_p}	Pressure Drag Coefficient
C_{D_f}	Skin Friction Drag Coefficient
C_P	Pressure Coefficient
C_L	Lift Coefficient

1. Objectives

The primary objective of testing aerofoils in a wind tunnel are to determine the aerodynamic polars of the aerofoils. The most important of which are the lift and drag polars which can be obtained using the simple experimental setup used in the lab, for NACA 0015 at $Re = 250{,}000$.

2. Experimental results

Tunnel operating conditions and model geometries:

Table 1: Experimental Conditions

Operating Conditions		Units
v	25.03	$[\mathrm{m/s}]$
T	23.1	$[°\mathrm{C}]$
ρ_{air}	1.19	$[\mathrm{kgm^{-3}}]$
$\rho_{ethanol}$	789.45	$[\mathrm{kgm^{-3}}]$
P_a	104,173	$[\mathrm{Pa}]$
c	15.24	$[\mathrm{cm}]$
Re	249,422	-
M	0.072285	-

2.1. Chord-wise Pressure Distribution

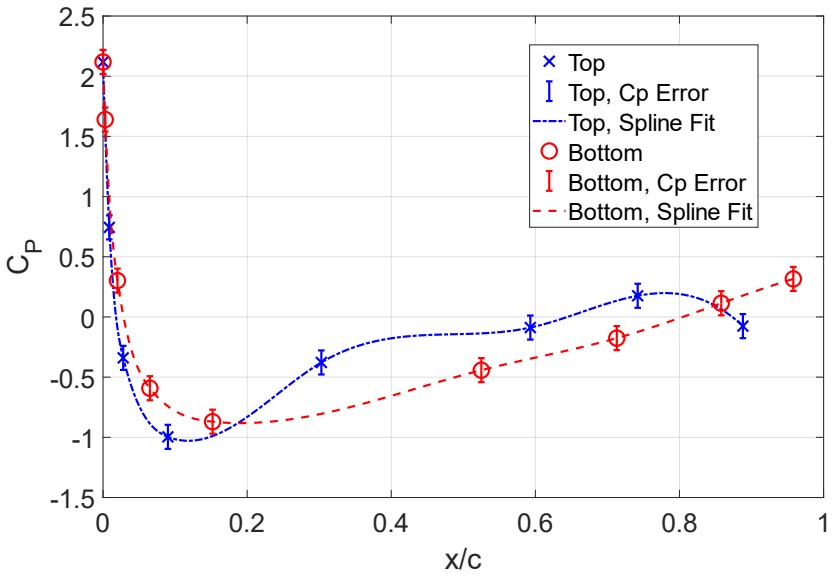

Figure 1: Chord-wise Pressure Distribution

The difference in the top and bottom C_P values indicate a higher pressure on the bottom of the aerofoil, indicative of a small amount of lift generation. This Lift is calculated via the Trapezoidal integration of these two curves to calculate the area between the curves. The Interpolation method used to fit the curve was a cubic spline method as it provides good curvature for the points at 0.1 on the chord. However, the spline fit introduces some wavy overfitting on the almost linear region of the plot between [0.2, 1.0].

2.2. Thickness-wise Pressure Distribution

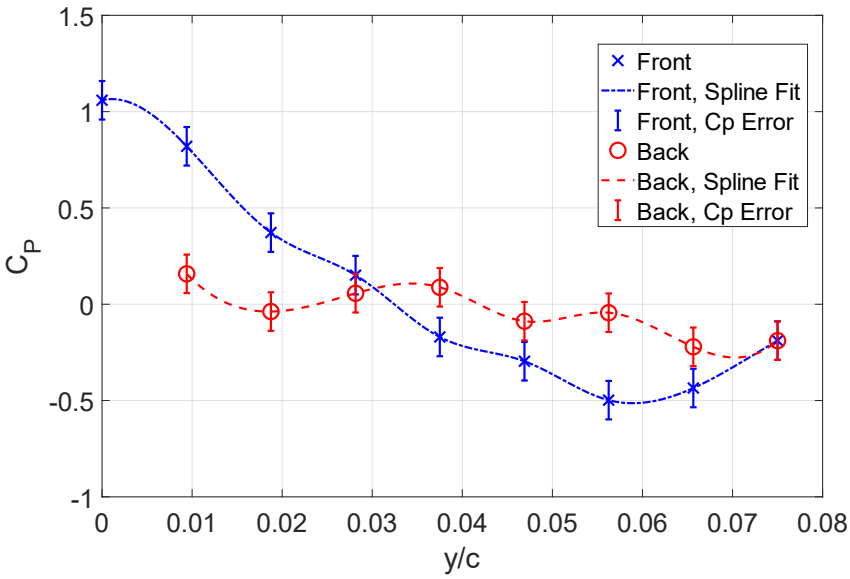

Figure 2: Thickness-wise Pressure Distribution

The difference in area between the lines represents the pressure drag on the aerofoil, which is calculated by trapezoidal integration. The fit used was cubic spline interpolation to allow the representation of the smoothness of the distribution to show. However, the mostly linear regions between [0.01,0.05] are overfitted and are excessively wavy.

2.3. Wake Momentum Deficit Profile

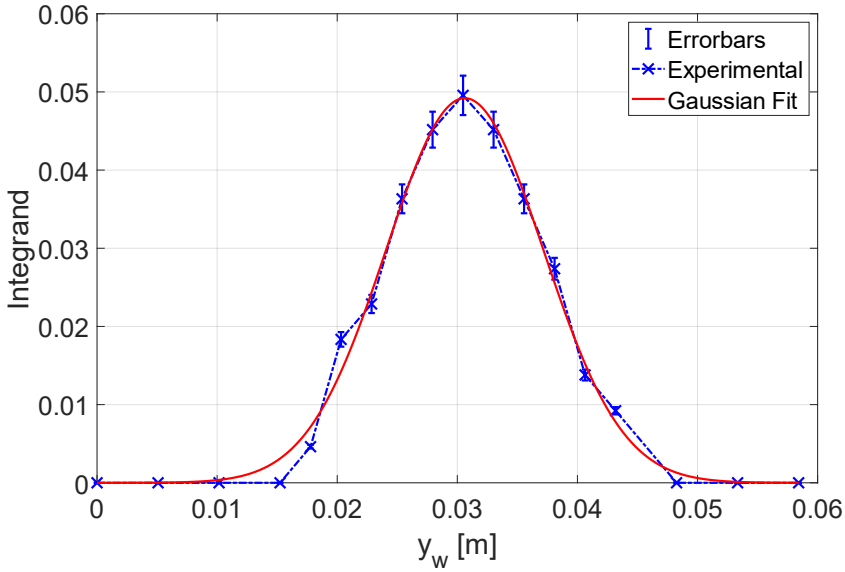

Figure 3: Integrand Plot

The Intergrand Plot Represents the Momentum Deficit in the Wake shown in equation (1) and is used to calculate C_D. A Gaussian fit was used to fit the distribution of the wake this was done to simplify the area calculations and compare the C_D from a trapezoidal integration scheme compared to fitting the analytical equation. The Gaussian fit well approximates the plot peak however fails to replicate the experimental results along the region between [0.01, 0.02]. a line connecting data points is also represented to show the effective area calculated by the Trapezoidal scheme is similar to the Gaussian.

2.4. Integrated Experimental Aerodynamic Coefficients

Table 2: Coefficients

Integration Method	C_D	C_{D_p}	C_{D_f}	C_L
Trapezoidal	0.01045 ± 0.0009	0.0073	0.0032	-0.10142
Gaussian	0.01059 ± 0.0010	0.0073	0.0033	-0.10142

Profile Drag is calculated using the formula:

$$C_D = \frac{2}{c}\int \left(\frac{H_W - p_\infty}{H_\infty - p_\infty}\right)^{\frac{1}{2}} \left(1 - \left(\frac{H_W - p_\infty}{H_\infty - p_\infty}\right)^{\frac{1}{2}}\right) dy_w \tag{1}$$

(1)

From the experimental data, two methods were used to find the integral. Firstly, using a First Order Gaussian fit, which is commonly used to fit peaks, yields the fit equation:

$$f(x) = a_1 e^{\left(-\left(\frac{x-b_1}{c_1}\right)^2\right)} \tag{2}$$

Table 3: Gaussian Fit Parameters

Parameters	95% confidence Bounds
$a_1 = 0.04920$	(0.04705, 0.05135)
$b_1 = 0.03062$	(0.03029, 0.03095)
$c_1 = 0.00925$	(0.008771, 0.009729)

The C_D is given from the model empirically by:

$$C_D = \frac{2}{c}\left(a_1 c_1 \sqrt{\pi}\right) = 0.01059 \pm 0.0010 \tag{3}$$

Using the Trapezoidal Integration technique and the existing data points yields the value of

$$C_D = 0.01045 \pm 0.0009$$

3. Error analysis

The accuracy of all measurement instruments is recorded in the table. The error Propagation for the pressure drag is calculated via the error propagation of U_{C_P} The total Drag Coefficient is outlined below and the subsequent integral errors are calculated.

3.1 Error Propagation

Error propagation table of associated errors for instruments and formulas used

Table 4: Measurement Errors

Instrument/Quantity	Symbol	Measurement error (±)	Units
Manometer height scale	U_h	1	$[\mathrm{mm}]$
Manometer angle gauge	U_θ	0.5	$[°]$
Wind tunnel Velocity	U_v	0.005	$[\mathrm{m/s}]$
Pressure Coefficient	U_{C_P}	-	$[\mathrm{Pa}]$

Via error propagation of summing the squares we arrive at the formula below:

$$U_{C_P} = \sqrt{(U_h)^2\left(\frac{2gsin(\theta)}{v^2}\right)^2 + (U_v)^2\left(\frac{4hgsin(\theta)}{v^3}\right)^2 + (U_\theta)^2\left(\frac{2hgcos(\theta)}{v^2}\right)^2} \tag{4}$$

3.2 Integration Error

For the Gaussian fit, upper and lower 95% confidence bounds were given for each parameter value in Table 3. Hence the error in the C_D can be given by:

$$U_{C_D} = \frac{1}{2}\left(\frac{2}{c}\left(a_{upper}c_{upper}\sqrt{\pi}\right) - \frac{2}{c}\left(a_{lower}c_{lower}\sqrt{\pi}\right)\right) = \pm 0.0010$$

For the Trapezoidal integration scheme on $[y_{w_a}, y_{w_b}]$ with n strips, the error is given by:

$$U_{C_D} = \frac{2}{c}\frac{\left(y_{w_b} - y_{w_a}\right)^3}{12n^2} max\left(f''(x)\right) \quad (5)$$

Assuming a Gaussian fit for simplifications, $max(f''(x)) = \frac{2a_1}{{c_1}^2}$

$$U_{C_D} = \frac{2}{c}\frac{\left(y_{w_b} - y_{w_a}\right)^3}{12n^2}\left(\frac{2a_1}{{c_1}^2}\right) = \pm 0.0009$$

4. Discussions

4.1. Forms of Drag

Multiple forms of Drag occur, however the most dominant in this region of flow are Pressure and Skin Friction Drag.

4.1.1. Pressure Drag

The Pressure Drag occurs due to the pressure difference between the front and back of the aerofoil geometry. Caused by the component of the pressure force perpendicular to the surface acting in the chordwise direction. The Pressure Drag Coefficient is calculated by trapezoidal integration of Figure 2 using the below equation (6).

$$C_{D_p} = \int\left(C_{P_F} - C_{P_R}\right)d\left(\frac{y}{c}\right) \quad (6)$$

Where $C_{P_F}$and C_{P_R} are the front and Rear Pressure Distributions respectively.

4.1.2. Skin Friction Drag

The Skin Friction Drag occurs due to the wall shear forces parallel to the surface acting on the fluid flow in the boundary layer of the aerofoil. These shear forces arise due to viscous flow around the aerofoil and the no-slip condition on the aerofoil surface. Skin Friction Drag Coefficient is calculated by (7).

$$C_{D_f} = C_D - C_{D_p} \quad (7)$$

Where C_D is the total drag calculated from the Wake of the Aerofoil.

5. Numerical results

5.1. Solver Setup, Parameters and Tunnel Conditions

The model was set up using version 2206 of SIEMENS Simcenter STAR-CCM+ from 2022, and part and tunnel geometries were provided. The solver setup used is provided in Figure 4. The parameters and tunnel conditions used are summarised in Table 5.

Table 5: Model Parameters

Simulation Parameters		Units
v	25.03	$[\mathrm{m/s}]$
T	23.1	$[^{\circ}\mathrm{C}]$
ρ_{air}	1.19	$[\mathrm{kg\ m^{-3}}]$
P_a	104,173	$[\mathrm{Pa}]$
c	15.24	$[\mathrm{cm}]$
Re	249,422	-
Turbulence Intensity	0.002	-
k (Turbulent Kinetic Energy)	0.003759	-
Turbulent Length Scale	0.028956	-

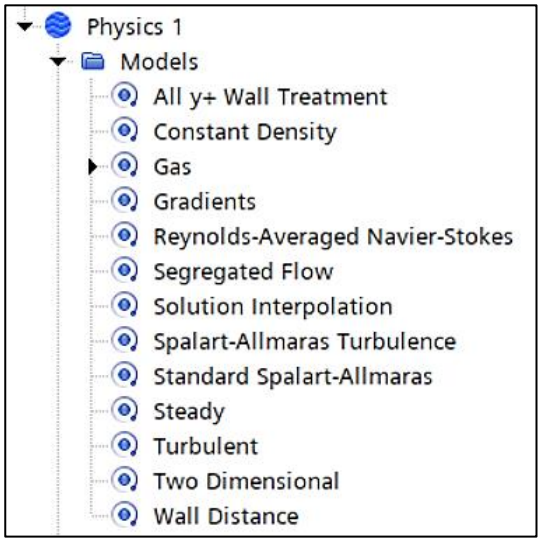

Figure 4: Solver Setup

5.2. Mesh Grid Independence Study

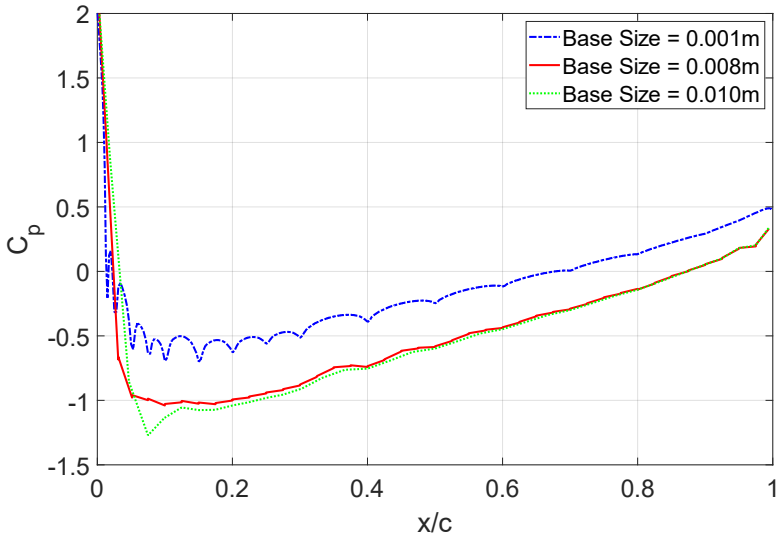

Figure 5: Pressure Distribution Base Size Study

The average pressure distribution along the x-axis from the CFD was calculated by averaging the top and bottom pressure values along the aerofoil surface. The plots show similarities to the top and bottom distribution of the experimental results and are indicative that the mean pressure values fall within the bounds of the curves in Figure 1 for base sizes 0.001m and 0.008m but are outside of the range for base size of 0.010m.

Table 6: Aerodynamic Forces From StarCCM+

Base Size [m]	C_L	C_D	C_{D_p}	C_{D_f}
0.001	-0.001752059	0.045398009	0.020156083	0.025241926
0.008	-0.001752028	0.045277466	0.020222744	0.025054723
0.010	-0.001754807	0.045297251	0.020234467	0.025062785
0.100	-0.001754432	0.050986635	0.020246419	0.030740216
Average	**-0.001752965**	**0.045324242**	**0.020204431**	**0.025119811**

Note: Base Size = 0.100m is not included in the Average values.

The Mesh Grid Independence Study was conducted with the Base Sizes listed and provided sufficiently close values for a range of Base sizes between 0.010-0.001m, which indicates grid independence for this range. The average was then taken to compare with the experimental values.

5.3. Simulation Results

Table 7: Comparison of Results

Method		C_D	C_{D_p}	C_{D_f}	C_L
Experimental	Trapezoidal	0.01045 ± 0.0009	0.0073	0.0032	-0.10142
	Gaussian	0.01059 ± 0.0010	0.0073	0.0033	-0.10142
CFD	Average	0.04532	0.0202	0.0251	-0.00175

The Experimental Data collected varies vastly in comparison to the CFD data in all aspects. The CFD results predict Skin friction Drag to be the dominant drag, which is expected due to the thin aerofoil shape. However, experimental results contradict this hypothesis due to the presence of Higher pressure drag compared to skin friction drag. This is most likely an error in the experimental results which may have been influenced by the 3D-wing effects which become more prominent in the larger wind tunnel.
Overall, the Experimental data predicts an almost 400% increase in total drag for the CFD study compared to the experimental data. There is additionally an order of magnitude difference in the skin friction and pressure drag between the CFD and Experimental results respectively

6. Conclusions

Experimental Improvements

- Use of a Smaller Wind tunnel to better mitigate 3D Wing effects
- Use of Digital Manometer to increase precision and negate human error
- Use of turning wheel for more precise angle setting
- Resting the Manometer on a level surface to allow for consistent ambient height readings

Numerical Simulation Improvements

- Use of a model with movable angle of attack to help better set zero lift AOA in the simulation.
- Use of multiple solvers better suited to Turbulent and Transition flow regains to better approximate the Boundary layer as the RANS (Reynolds Averaged Navier Stokes) Solver may perform worst in the Flow Regime compared to a more complex LES or DNS solver.